Journal of Statistical Physics, Vol. 90, Nos. 5/6, 1998

Two-Dimensional Oriented Self-Avoiding Walks with Parallel Contacts

G. T. Barkema,[1,2] U. Bastolla,[1] and P. Grassberger[1]

Received August 8, 1997; final November 25, 1997

Two closely related models of oriented self-avoiding walks (OSAWs) on a square lattice are studied. We use the pruned-enriched Rosenbluth method to determine numerically the phase diagram. Both models have three phases: a tight-spiral phase in which the binding of parallel steps dominates, a collapsed phase when the binding of antiparallel steps dominates, and a free (open coil) phase. We show that the system features a first-order phase transition from the free phase to the tight-spiral phase, while both other transitions are continuous. The location of the phases is determined accurately. We also study turning numbers and gamma exponents in various regions of the phase diagram.

KEY WORDS: Self-avoiding walks; oriented walks; collapse; spiral walks; Monte Carlo; theta transition.

I. INTRODUCTION

Many aspects of the behavior of polymers can be described by self-avoiding walks on a lattice. To incorporate the interactions of the polymer with itself, a binding energy ε can be assigned if either two nearest-neighbour lattice sites are visited by the polymer (point-contact model), or if two steps of the SAW are located on opposite sides of a plaquette of the lattice (step-contact model). Both models show the same qualitative behaviour.

To describe the coil-globule ("theta") transition, it is sufficient to assume these interactions to be isotropic, but some polymers have interactions that depend on the spatial orientation of the polymer, for instance A-B polyester. Such polymers are conveniently modeled by *oriented* self-avoiding walks (OSAW) with short-ranged interaction between steps

[1] HLRZ, Forschungszentrum Jülich, D-52425 Jülich, Germany.
[2] ITP, Utrecht University, Princetonplein 5, 3584 CC Utrecht, The Netherlands.

0022-4715/98/0300-1311$15.00/0

depending on their relative orientation.[1-7] This orientation-dependent strength of the interaction can be incorporated in the model by distinguishing *parallel* and *anti-parallel* step-contacts, and assigning an *additional* binding energy ε_p only between parallel step-contacts; with point-contact energies, incorporating orientation-dependence in an elegant manner is complicated by the ends of the polymer.

Most research on SAWs has been based on the point-contact model, since it is numerically better behaved than the step-contact model. Most research on OSAWs however has been based on the step-contact model, in which the inclusion of the additional binding of parallel step-contacts is more natural to the model. We will study both models in this manuscript.

Bennett-Wood *et al.*[2] enumerated all configurations up to SAWs with a length of $n = 29$ and ordered them according to their number of parallel and anti-parallel step-contacts. These results showed the existence of three phases: a free SAW phase, a normal collapsed phase and a compact spiral phase. The transition from the free to the spiral phase was conjectured to be of first order.

For the case $\varepsilon = 0$ (only binding energies between parallel step-contacts), Barkema and Flesia[5] extended the exact enumeration of the OSAWs to length $n = 34$. In the same paper, the energy of the ground state (for positive ε_p) and its degeneracy as a function of length was given, and an approximation to the number of configurations $C_n(m_p)$ of polymers of length n with m_p parallel step-contacts was proposed:

$$\begin{aligned} C_n(1) &= p_n C_n(0) \\ C_n(m_p) &\approx C_n(1) \cdot \exp(-q_n(m_p - 1)) \qquad (m_p > 1) \end{aligned} \tag{1}$$

where p_n and q_n are n-dependent parameters. The partition function for $\varepsilon = 0$ can be constructed, and from this it was concluded that the transition from the free phase to the spiral phase at $\varepsilon = 0$ occurs at $\varepsilon_p = \log(\mu) = 0.9701$ (where $\mu = 2.638$ is the growth constant for SAWs[8]) and is a first order transition. We use units such that $k_B T = 1$.

For the step-contact model, Prellberg and Drossel[6] argued that the transition from the collapsed phase to the spiral phase is continuous. They also argued that the location of the theta-transition (from the free to the collapsed phase) is independent of ε_p.

Trovato and Seno[7] performed transfer matrix calculations on the point-contact model. They also made some calculations for the step-contact model, but with much less conclusive results. They found that the transition from either the free or the collapsed to the spiral phase is probably of first order.

In this paper, we employ the pruned-enriched Rosenbluth method (PERM)[9-11] to study the phase diagram of both models for two-dimensional OSAWs. The only deviation from the algorithm as described in the above references is that new steps were biased both towards large numbers of contacts and large absolute values of the turning number, with different biases in different parts of the phase diagram. As usual in PERM, this is corrected for by reweighting.

The manuscript is organized as follows. In Section II we study the phase transition from the free phase towards the spiral phase in the step-contact model. To do this, we determine numerically the partition function along three lines $\varepsilon = \text{constant}$, for all ε_p.

In Section III, we use the same technique as in Section II to study the transition from the collapsed to the spiral phase, but for different values of ε which are above the collapse energy ε_θ.

The next section, Section IV, studies the transitions for ε close to the collapse point ε_θ. To do this, we use the point-contact model, since for this model finite-size corrections at $\varepsilon = \varepsilon_\theta$ are smaller, and simulations using PERM have smaller statistical fluctuations.

In Section V, we present our numerically determined phase diagram for both models, discuss the nature and location of all phase transitions, and summarize the results.

II. TRANSITION FROM THE FREE PHASE TO THE SPIRAL PHASE

With PERM, we measured $C_n(m_p)$, the contribution to the partition function for walks of n steps from configurations with m_p parallel contacts. First, we did this at $\varepsilon = 0$, so that we can compare our results with previous work. In Fig. 1 we have plotted $\log(C_n(m_p))$ as a function of m_p for various chain lengths n. To a good approximation, the curves are straight lines, in agreement with the guess Eq. (1). The inset shows the deviation from the straight line for $n = 256$, by plotting $\log(C_n(m_p)) + 1.229 m_p$. The figure combines data obtained at several values of ε_p close to the transition.

From the partition function plot we conclude that there is a first-order transition from the free phase, where configurations with no parallel contacts dominate, to the spiral phase, where configurations with many parallel contacts dominate. A closer look shows that the curves in Fig. 1 are not completely straight but S-shaped, with a "bump" at some number m_b^* of parallel contacts. Looking at increasing lengths n of the OSAWs, we see no evidence that asymptotically $m_b^*/n \to 0$ nor $m_b^*/n \to 1$, and therefore conclude that this bump will persist in the thermodynamic limit ($n \to \infty$). To extract the transition temperature $\varepsilon_{p,\,\text{crit}}(n)$, we have determined for

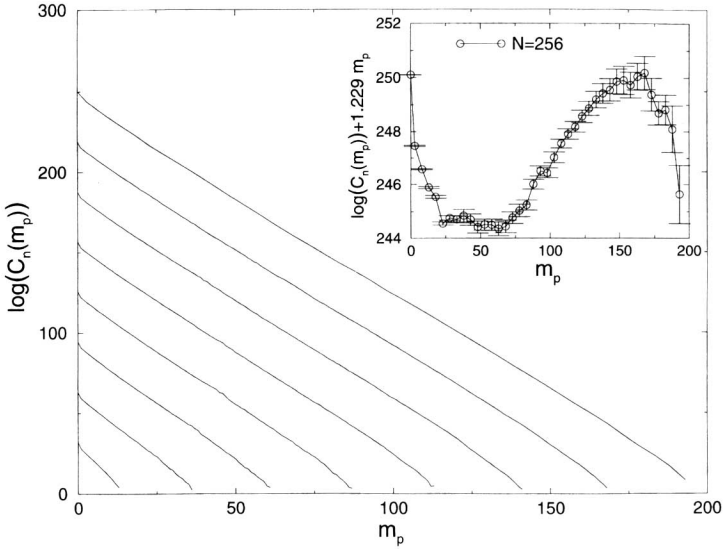

Fig. 1. Logarithm of the contribution to the partition function $C_n(m_p)$ of configurations with m_p parallel contacts, in the absence of anti-parallel interactions (i.e., $\varepsilon = 0$). The lines correspond to chain lengths of $n = 32, 64, ..., 256$ steps. The inset shows the deviation from a straight line, by plotting $\log(C_{256}(m_p)) + 1.229 m_p$ as a function of m_p. The presence of two peaks indicates a first-order phase transition.

which ε_p the top of the bump and the walks with no parallel contacts contribute equally to the partition function. The results are $\varepsilon_{p,\,\mathrm{crit}}(n) = 2.11(3)$, 1.6(1), 1.42(4), 1.368(7), 1.315(2), 1.278(2), 1.250(2); and 1.229(2) for $n = 32, 64, ..., 256$ respectively.

Since the number of parallel contacts in a tight spiral scales as $n - 4\sqrt{n}$, we expect corrections of order $n^{-1/2}$ to the critical temperature. Most likely, there are also corrections of order n^{-1}, and possibly other corrections. Assuming however that corrections of order $n^{-1/2}$ are the leading ones, we extrapolated our values for $\varepsilon_{p,\,\mathrm{crit}}(n)$ to the limit $n \to \infty$, and obtained for $\varepsilon = 0$ in the thermodynamic limit $\varepsilon_{p,\,\mathrm{crit}} = 0.90(5)$, with the error mainly due to the uncertainty in the finite-size correction.

We also studied the contribution to the partition function as a function of the turning number t: the number of turns that the walk has made clockwise, minus the number of turns anti-clockwise. Note that the turning number is not equal to the winding number w as defined by Duplantier and Saleur;[12] for large chains in the free and the collapsed phase however, the two quantities are related by $\langle((\pi/2)\, t)^2\rangle = 2\langle w^2\rangle$. The factor of two is explained by observing that the turning number receives contribution from both ends of the chain, while only one end contributes to the winding

number.[13] For the spiral ground state, the turning number is roughly equal to $2\sqrt{(n)}$.

Results for $n=256$ are presented in Fig. 2, where we averaged the histograms for positive and negative turning numbers. We observe that for $\varepsilon_p = 1.253$, the histogram has two peaks at ± 23: we are in the spiral phase. At $\varepsilon_p = 0$, the turning number is between -10 and 10, with a maximum at zero: we are outside the spiral phase. At $\varepsilon = 1.194$ we are close to the transition, and the peaks at $t = \pm 21$ and the peak around zero coexist. The fact that in the histogram for turning numbers the peaks maintain their location, while their relative importance changes, is consistent with our earlier conclusion that the phase transition is first-order. For a continuous transition, we would expect that the two peaks in the spiral phase would approach zero gradually.

We repeated this procedure for $\varepsilon = 0.993$ and for the case where anti-parallel contacts are strictly forbidden ($\varepsilon \to -\infty$) but parallel contacts have a finite binding energy ($\varepsilon + \varepsilon_p$ is finite). Qualitatively, the behavior is the same as for $\varepsilon = 0$, and we conclude that the transition is also first-order. The bump seems to shift to the left with increasing ε. For $\varepsilon = 0.993$ we obtained in the thermodynamic limit $\varepsilon_{p,\,\mathrm{crit}} = 0.05(5)$, while if anti-parallel contacts are strictly forbidden, we find $\varepsilon_{p,\,\mathrm{crit}} + \varepsilon = 0.75(5)$.

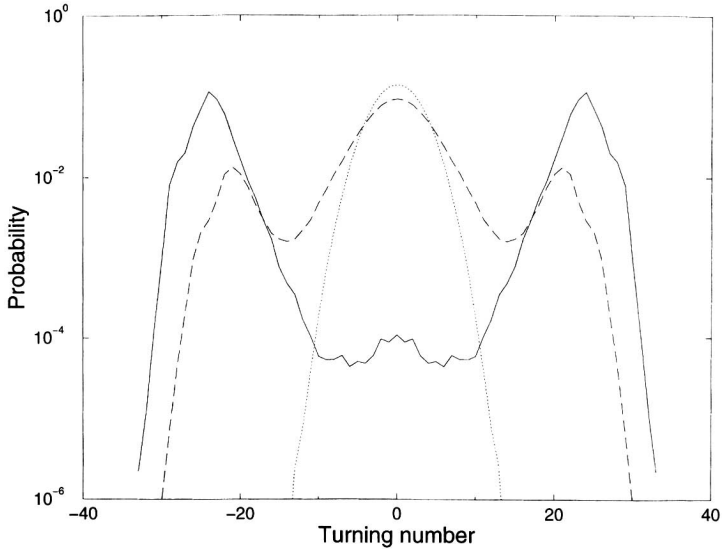

Fig. 2. Probability of turning number t as a function of t, for chains of length $n=256$ for the case $\varepsilon = 0$. Different curves correspond to $\varepsilon_p = 0$ (dotted line), $\varepsilon_p = 1.194$ (dashed line), and $\varepsilon_p = 1.253$ (solid line).

III. TRANSITION FROM THE COLLAPSED PHASE TO THE SPIRAL PHASE

To study the transition from the collapsed phase to the spiral phase in the step-contact model, we used the same technique as in Section II: at a particular value for ε, we calculated the contribution of configurations to the partition function as a function of the number of its parallel contacts. This allows us to determine both the nature and the location of the phase transition at the particular value of ε.

We used this method for $\varepsilon = 1.253$, 1.435 and 1.609. These values are well above the theta-transition, which is estimated to be $\varepsilon = 1.21$ (see Section IV). Results analogous to those shown in Fig. 1, but now for $\varepsilon = 1.609$, are presented in Fig. 3. There are still two maxima in the histogram—one at $m_p = 0$ and the other at $m_p^* > 0$—but the valley between them is very shallow and much more narrow. Comparison of different chain lengths now suggests that in the thermodynamic limit m_p^*/n approaches zero, indicating that the transition has become continuous.

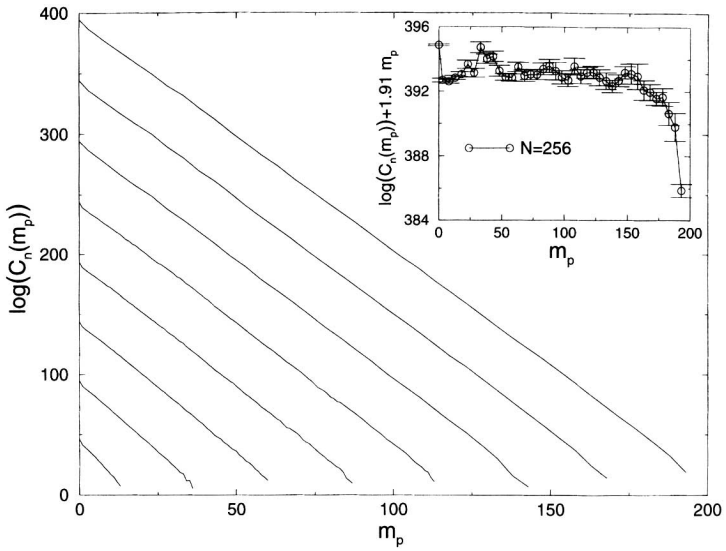

Fig. 3. Logarithm of the contribution to the partition function $C_n(m_p)$ of configurations with m_p parallel contacts, for the case $\varepsilon = 1.609$ and no interaction between parallel steps ($\varepsilon + \varepsilon_p = 0$). Different curves correspond to chain lengths $n = 32, 64, ..., 256$ steps. The inset shows the deviation from the straight line by plotting $\log(C_{256}(m_p)) + 1.91 m_p$ as a function of m_p. The two peaks that were present in the case $\varepsilon = 0$ have nearly disappeared and are compatible with being finite size effects, indicating that the first-order phase transition has changed into a continuous one.

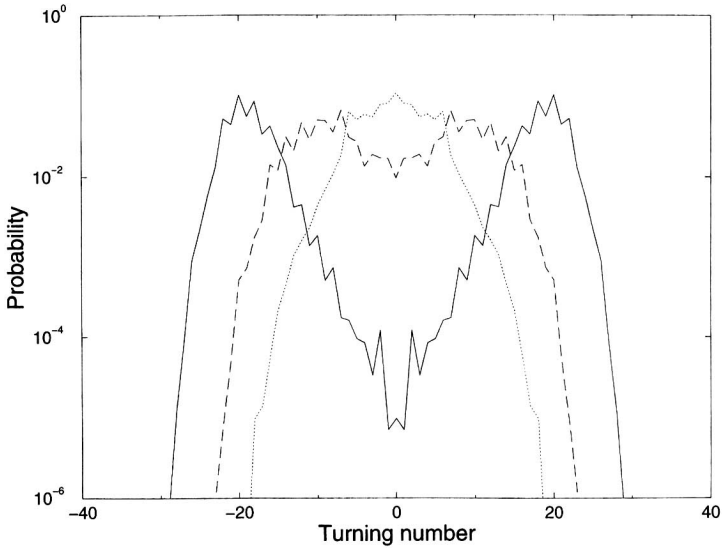

Fig. 4. Probability of turning number t as a function of t, for chains of length $n = 256$, in the case $\varepsilon = 1.609$. Different curves correspond to $\varepsilon_p = 1.82$ (dotted line), 1.92 (dashed line), and $\varepsilon_p = 1.96$ (solid line).

We obtained estimates for the location of the phase transition line that are consistent with $\varepsilon_{p,\,\mathrm{crit}} = 0$.

The histogram of the turning numbers is plotted in Fig. 4. The picture is quite different from that of Fig. 2: the peaks at high positive and negative turning numbers do not maintain their location if the transition line is approached, but shift towards zero, where they merge. This is consistent with a continuous phase transition.

IV. TRANSITION FROM THE FREE TO THE COLLAPSED PHASE

At first, we simulated the step-contact model at various values of ε, to obtain a precise value of ε_θ. Requiring that the end-to-end distance scales as $n^{4/7}$ and the partition sum as $\mu_\theta^n n^{1/7}$ (see Duplantier and Saleur[14]), we got $\varepsilon_\theta = 1.21(2)$, independent of the value of ε_p, as long as $\varepsilon_p < 0$. Next, we simulated the ordinary (non-oriented) point-contact model at various values of ε, to obtain a precise value of ε_θ and we got $\varepsilon_\theta = 0.667(1)$, in good agreement with earlier estimates.[15, 16]

This difference in ε_θ is due to the fact that point contacts are roughly twice as frequent as bond contacts near the theta point, and it makes

simulations in the regime $\varepsilon \geqslant \varepsilon_\theta$ much harder in the step-contact model than in the point-contact model: due to the large value of ε, the Boltzmann weights of different configurations fluctuate strongly, which creates problems for PERM. The point-contact model can be simulated more efficiently by PERM (error bars decrease by roughly one order of magnitude for the same CPU times), and systematic errors due to finite-size corrections decrease, although they stay sizeable in both models (the same was found by Trovato and Seno[7] for transfer matrix calculations).

For this reason we used the point-contact model to study transitions for $\varepsilon \approx \varepsilon_\theta$ in detail. This includes the coil-globule transition for $\varepsilon_p < 0$ which happens exactly at $\varepsilon = \varepsilon_\theta$, as well as the region around the triple point $(\varepsilon = \varepsilon_\theta, \varepsilon_p = 0)$.

In the same runs we also measured the average number of parallel contacts. Results are shown in Fig. 5. They indicate that $\langle m_p \rangle$ converges for $n \to \infty$ to a finite value, in agreement with Barkema and Flesia,[5] as long as $\varepsilon < \varepsilon_\theta$. This is however no longer true for $\varepsilon \geqslant \varepsilon_\theta$. Exactly at the θ-point, $\langle m_p \rangle$ increases roughly as $\sqrt{n}$ for large n. But finite size corrections are so large that it is not clear whether this is really the asymptotic behavior. Thus, while parallel bonds are unimportant below the θ-point, they become important above it. Consistent with this, we found that the probability $P_n(0) = C_n(0)/\sum_m C_n(m)$ of having no parallel bond at all

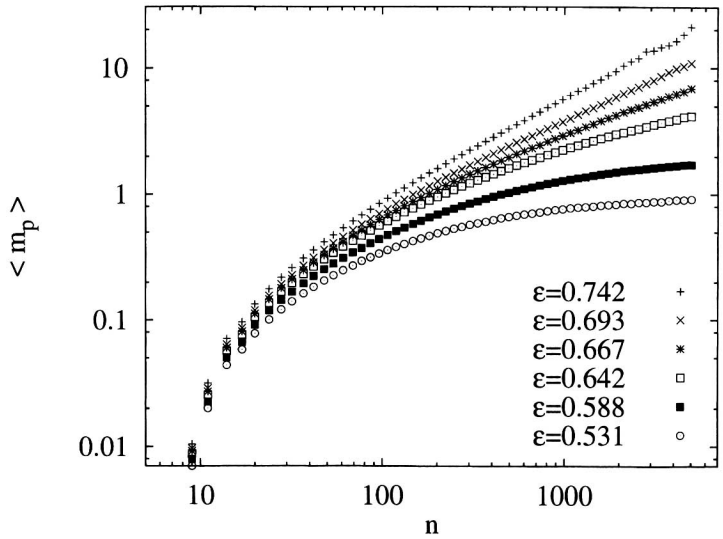

Fig. 5. Log-log plot of the average number of parallel bonds versus chain length for different values of ε, and for $\varepsilon_p = 0$. The θ-point is at $\varepsilon = 0.667$.

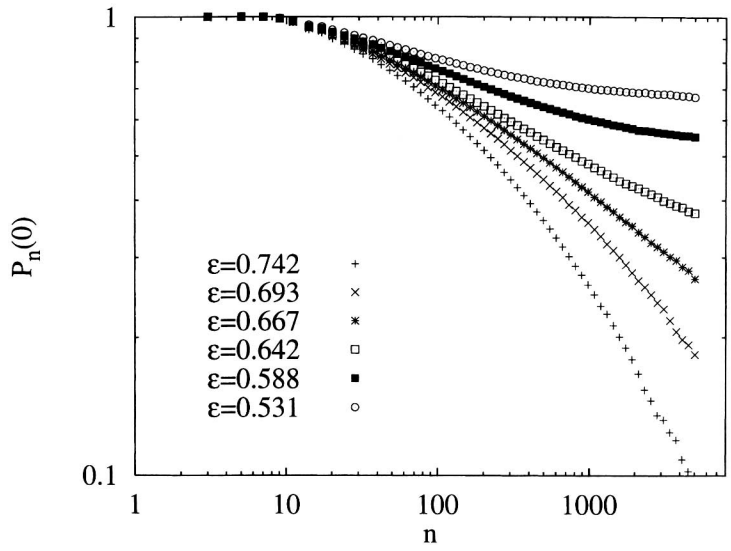

Fig. 6. Log-log plot of $P_n(0)$, the chance to have no parallel bonds in an n-step walk.

decreases to zero for $\varepsilon \geqslant \varepsilon_\theta$, while it converges to a finite value for $\varepsilon < \varepsilon_\theta$ (Fig. 6). Based on the analogy with parts of percolation cluster hulls, it was conjectured by Prellberg and Drossel[6] that $P_n(0) = n^{-2/7}$ exactly at the θ-point. This is consistent with our data, although our data show again very slow convergence and would suggest an exponent $\approx 1/4$ rather than 2/7.

The fact that $P_n(0)$ does not decrease exponentially with n for $\varepsilon < \varepsilon_\theta$ shows that indeed the open coil/globule collapse occurs for all $\varepsilon_p < 0$ at the same value of ε, namely $\varepsilon = \varepsilon_\theta$.[2, 6, 7] Parallel contacts are simply too rare to effect phase boundaries for $\varepsilon_p < 0$. On the other hand, the fact that $\langle m_p \rangle$ diverges at ε_θ implies that this is no longer true for $\varepsilon_p > 0$. Thus the phase boundary has a singularity at $(\varepsilon, \varepsilon_p) = (\varepsilon_\theta, 0)$, which suggests that this point is indeed the triple point where all three phase boundaries meet.[7]

In order to verify this and to determine the orders of the coil-spiral and globule-spiral transitions, we measured also the distribution

$$P_n(m_p) = C_n(m_p) \Big/ \sum_m C_n(m) \tag{2}$$

Typical results for $\varepsilon < \varepsilon_\theta$ and for $\varepsilon > \varepsilon_\theta$ are shown in panels (a) and (b) of Fig. 7, respectively. While $P_n(m_p)$ decreases roughly exponentially with m_p in both plots, details are rather different. In panel (a) the exponent is nearly independent of n, suggesting that it is nonzero also for $n \to \infty$. Thus, the free-spiral transition happens at a positive ε_p. In contrast, the exponent

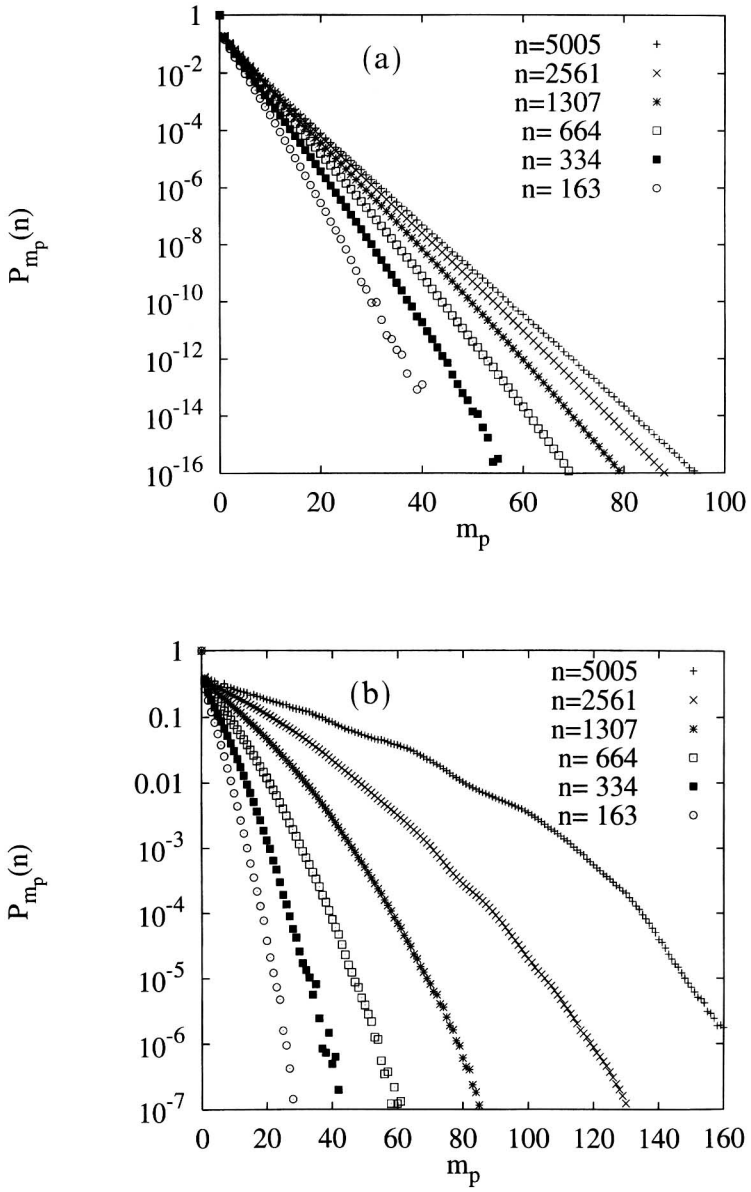

Fig. 7. Distributions $P_n(m_p)$ for finding m_p parallel bonds in chains of length n, normalized to $P_n(0) = 1$. Each panel contains curves for $n = 163$, 334, 664, 1307, 2561, and 5005. Panel (a) is for $\varepsilon = 0.531 < \varepsilon_\theta$, while panel (b) is for $\varepsilon = 0.742 > \varepsilon_\theta$.

depends strongly on n in panel (b), and seems to converge to zero for $n \to \infty$. This is confirmed by a more careful analysis. It shows that the collapsed-spiral transition happens exactly at $\varepsilon_p = 0$, as suggested by Trovato and Seno.[7]

To determine the order of the transitions, we plot $e^{a(\varepsilon) m_p} P_n(m_p)$ with the parameter $a(\varepsilon)$ determined such that both peaks in this function have the same height (compare the inserts in Figs. 1 and 3). This is done for several values of ε, but only for a single chain length ($n = 2561$). Again the data are normalized to $P_n(0) = 1$. Results are shown in Fig. 8. We see that there are two peaks for all values of ε, but that the right peak is located at very small values of m_p in the collapsed region, and moves to larger values of m_p only if we go with ε below the θ-point. Thus we see again that the double peak structure is a finite-size effect in the collapsed phase, as we had already seen in Section III, and that the collapse-to-spiral transition is second order.

Finally, we also measured turning numbers at and near $\varepsilon = \varepsilon_\theta$. Average squared turning numbers at the triple point $(\varepsilon, \varepsilon_p) = (\varepsilon_\theta, 0)$ and at the point $(\varepsilon_\theta, -\infty)$ are shown in Fig. 9. Apart from the by now familiar large deviations for small n, we see clear indications for logarithmic laws $\langle ((\pi/2)\, t)^2 \rangle = 2 \langle w^2 \rangle = 2C \log n$. The constants C are fully compatible with the predictions $C = 24/7$ at $(\varepsilon_\theta, 0)$[12] and 6/7 at $(\varepsilon_\theta, -\infty)$[6] which are

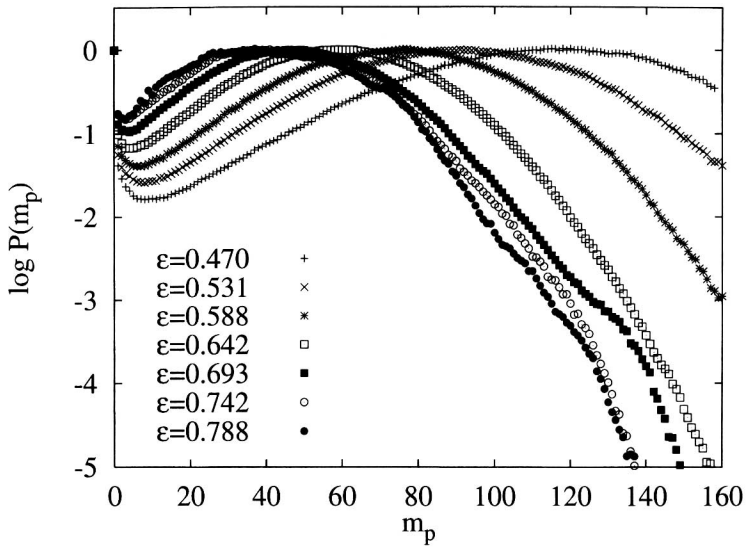

Fig. 8. Log-log plot of $e^{a(\varepsilon) m_p} P_n(0)$, with $a(\varepsilon)$ such that both peaks have the same height. Again normalization is such that $P_n(0) = 1$.

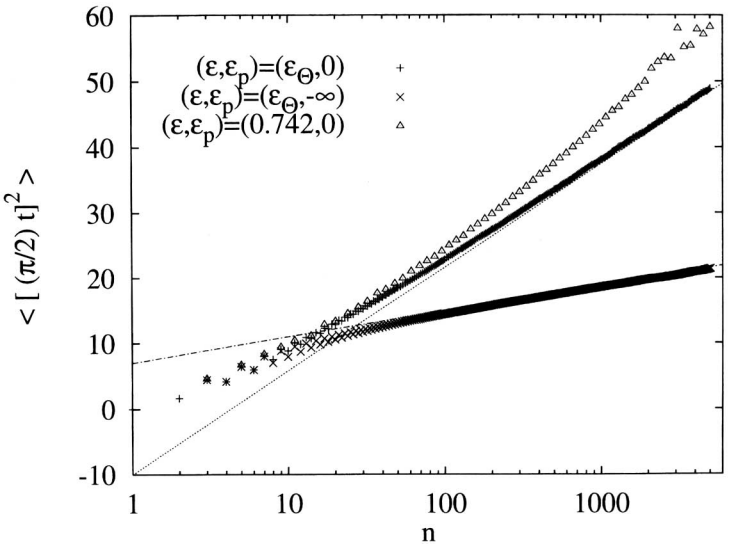

Fig. 9. Average squared turning number $\langle t^2 \rangle$ against $\log n$, for $(\varepsilon, \varepsilon_p) = (\varepsilon_\theta, 0)$ (+), $(\varepsilon_\theta, -\infty)$ (×), and (0.742, 0) (△). The straight lines are the theoretical predictions for the first two cases.

indicated in Fig. 9 by straight lines. We have not measured turning numbers with similar precision in other phases, but the overall picture seems fully compatible with that of Prellberg and Drossel.[6] On the collapsed-spiral transition line ($\varepsilon > \varepsilon_\theta, \varepsilon_p = 0$), $\langle t^2 \rangle$ seems to increase faster than $\log n$ (see also Fig. 9), but our data are less precise there.

V. CONCLUSIONS AND DISCUSSION OF THE PHASE DIAGRAM

We have found three phases for two-dimensional OSAWs: two of them, the free phase and the collapsed phase, also exist in normal SAWs, and have a turning number around zero; the third phase, the spiral phase, is unique for OSAWs, and has a high turning number.

In Section IV, we have confirmed that the location of the transition from the free to the collapsed phase is independent of the strength of parallel interactions. The critical value is estimated to be $\varepsilon_\theta = 1.21(2)$ for the step-contact model, and $\varepsilon_\theta = 0.667(1)$ for the point-contact model. This transition also exists for SAWs, and is known to be continuous.

The transition from the collapsed to the spiral phase is found to be also continuous, and located at $\varepsilon_p = 0$, in agreement with theoretical predictions.[6]

In Section II, we concluded that the transition from the free phase to the spiral phase is a first-order one. For the step-contact model, we have located three points $(\varepsilon + \varepsilon_p, \varepsilon)$ on the phase transition line: $(0.75, -\infty)$; $(0.90, 0)$, and $(1.04, 0.993)$. The results for the step-contact model are combined in Fig. 10, where the phase diagram of the step-contact model is presented. The phase diagram for the point contact model is identical except for the detailed location of the transition lines.

The probability $P_n(0)$ of hating no parallel bond at all decreases to zero for $\varepsilon \geqslant \varepsilon_\theta$, while it converges to a finite value for $\varepsilon < \varepsilon_\theta$. Exactly at the theta-point, it was conjectured by Prellberg and Drossel[6] that $P_n(0) = n^{-2/7}$. This is consistent with our data, although slightly smaller exponents are not ruled out.

At the triple point $(\varepsilon, \varepsilon_p) = (\varepsilon_\theta, 0)$ and at the point $(\varepsilon_\theta, -\infty)$, the average squared turning numbers grow logartihmically with n with constants as predicted by Duplantier and Saleur,[12] and Prellberg and Drossel.[6]

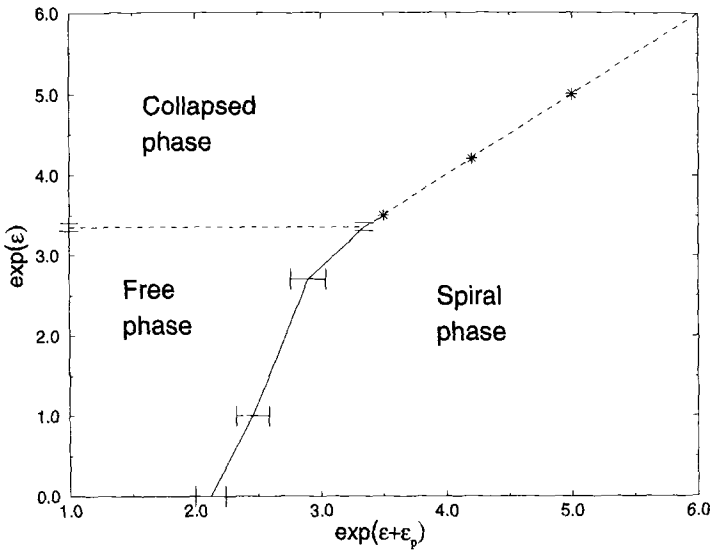

Fig. 10. Schematic drawing of the phase diagram of the step-contact model. The model has three phases, a free phase, a collapsed phase, and a spiral phase. The transitions from the collapsed phase to the free or the spiral phase are continuous, the transition from the free to the spiral phase is of first order. The transition line from the collapsed to the spiral phase is located at $\varepsilon_p = 0$. The transition from the free to the collapsed phase is located at $\varepsilon = 1.21(2)$. We determined three points on the transition line from the free to the spiral phase, and connected these points as a guide to the eye.

ACKNOWLEDGMENTS

GTB likes to thank S. Flesia for useful discussion. PG is supported by the Deutsche Forschungsgemeinschaft through SFB 237.

REFERENCES

1. J. L. Cardy, *Nucl. Phys. B.* **419**:411 (1994).
2. D. Bennet-Wood, J. L. Cardy, S. Flesia, A. J. Guttmann, and A. L. Owczarek, *J. Phys. A* **28**:5143 (1995).
3. S. Flesia, *Europhys. Lett.* **32**:149–154 (1995).
4. W. M. Koo, *J. Stat. Phys.* **81**:561 (1995).
5. G. T. Barkema and S. Flesia, *J. Stat. Phys.* **85**:363 (1996).
6. T. Prellberg and B. Drossel, *Phys. Rev. E* **57**:2045 (1998).
7. A. Trovato and F. Seno, *Phys. Rev. E* (1997).
8. A. Conway, I. G. Enting, and A. J. Guttmann, *J. Phys. A* **26**:1519 (1993).
9. P. Grassberger, *Phys. Rev. E* **56**:3682 (1997).
10. U. Bastolla and P. Grassberger, *J. Stat. Phys.* **89**:1061 (1997).
11. H. Frauenkron, U. Bastolla, E. Gerstner, P. Grassberger, and W. Nadler, cond-mat/9705146 (1997).
12. B. Duplantier and H. Saleur, *Phys. Rev. Lett.* **60**:2343 (1988).
13. For an OSAW from a starting point A to an end-point B, the turning number t_{AB} is related to the winding numbers w_{AB} (around A) and w_{BA} (around B) for the same OSAW by $(\pi/2)\, t_{AB} = w_{AB} - w_{BA} + \text{const}$, where $|\text{const}| < 4\pi$; independence of w_{AB} and w_{BA} for long walks leads then to $\langle((\pi/2)\, t)^2\rangle = 2\langle w^2\rangle$ in the asymptotic limit.
14. B. Duplantier and H. Saleur, *Phys. Rev. Lett.* **59**:539 (1987).
15. I. Chang and H. Meirovitch, *Phys. Rev. E* **48**:3656 (1993).
16. P. Grassberger and R. Hegger, *Journal de Physique I* **5**:597 (1995).